JOURNAL OF ENERGY, MATERIALS, AND INSTRUMENTATION TECHNOLOGY

Journal Webpage https://jemit.fmipa.unila.ac.id/

Strain-Tunable Anisotropic Rashba Splitting in Janus VSTe Monolayer: A First-Principles Study

Muhammad Anshory[1*], Yusron Darojat[1], Nadiisah Nurul Inayah[1], and Yusuf Affandi[2]

1. Department of Physics, Faculty of Science, Institut Teknologi Sumatera, Lampung Selatan, Indonesia, 35365
2. Instrumentation and Automation Engineering, Faculty of Industrial Technology, Institut Teknologi Sumatera, Lampung Selatan, Indonesia, 35365

Article Information

Article history:
Received April 19, 2026
Received in revised form May 4, 2026
Accepted May 5, 2026

Keywords: *density functional theory, janus VSTe, rashba splitting, spintronics, strain*

Abstract

This study investigates the Rashba effect in a Janus VSTe monolayer using first-principles density functional theory (DFT) calculations. We identify an anisotropic Rashba splitting near the Γ point in the first Brillouin zone, which is further analyzed through $\vec{k}\cdot\vec{p}$ perturbation theory and symmetry group analysis. Our work identifies a highly tunable anisotropic Rashba effect in Janus VSTe monolayer, revealing that third-order terms in the Hamiltonian play a critical role in governing its spin-splitting characteristics. Our results reveal that the first-order Rashba parameter (α_1) for the pristine Janus VSTe monolayer is 0.055 eVÅ along the $\Gamma - K$ path. Furthermore, biaxial strain engineering effectively modulates these characteristics, where a 5% expansive strain significantly enhances the Rashba splitting, reaching α_1 value of 0.095 eVÅ. These findings highlight the Janus VSTe monolayer as a promising candidate for next-generation spintronic devices, such as spin-field effect transistors, where controllable spin splitting is essential for device functionality.

Informasi Artikel

Proses artikel:
Diterima 19 April 2026
Diterima dan direvisi dari 4 Mei 2026
Accepted 5 Mei 2026

Kata kunci: *teori fungsional kerapatan, janus VSTe, pemisahan Rashba, spintronik, regangan*

Abstrak

Penelitian ini menyelidiki efek Rashba pada monolayer Janus VSTe menggunakan perhitungan prinsip pertama teori fungsional kerapatan (DFT). Kami mengidentifikasi adanya pemisahan Rashba anisotropik di sekitar titik Γ pada zona Brillouin pertama, yang selanjutnya dianalisis menggunakan teori perturbasi $\vec{k}\cdot\vec{p}$ dan analisis grup simetri. Penelitian kami menunjukkan adanya efek Rashba anisotropik yang sangat dapat diatur pada monolayer Janus VSTe, serta mengungkap bahwa suku-suku orde ketiga dalam Hamiltonian memainkan peran penting dalam mengatur karakteristik pemisahan spin. Hasil penelitian kami menunjukkan bahwa parameter Rashba orde pertama (α_1) untuk monolayer Janus VSTe murni adalah sebesar 0,055 eVÅ di sepanjang jalur $\Gamma - K$. Lebih lanjut, rekayasa regangan biaksial secara efektif dapat memodulasi karakteristik tersebut, dimana regangan ekspansif sebesar 5% mampu meningkatkan pemisahan Rashba secara signifikan hingga mencapai nilai α_1 sebesar 0,095 eVÅ. Temuan ini menegaskan bahwa monolayer Janus VSTe merupakan kandidat yang menjanjikan untuk perangkat spintronik generasi mendatang, seperti spin-field effect transistors, dimana pengendalian pemisahan spin sangat penting bagi fungsionalitas perangkat.

1. Introduction

The pursuit of next-generation spintronic devices has fueled intense research into materials that exhibit significant Rashba spin splitting [Manchon et al., 2015]. The Rashba effect is highly significant because its electrical tunability makes it a prime candidate for spintronic applications, such as spin-field effect transistors (S-FETs). These future transistors aim to overcome the performance and dimensional constraints of current technology by offering better energy efficiency and faster operating speeds. The performance of S-FETs relies on semiconductor materials

----
* Corresponding author.
E-mail address: muhammad.anshory@fi.itera.ac.id

that exhibit strong Rashba SOI, which facilitates spin precession and allows for the control of spin transport via gate voltage [Rao et al., 2023]. Strong Rashba SOI is particularly desirable as it enables devices to function at room temperature. The Rashba phenomenon, arising from the lifting of spin degeneracy due to broken inversion symmetry and strong spin-orbit coupling (SOC), allows for the electrical manipulation of spin states without the need for an external magnetic field [Bychkov and Rashba, 1984].

Theoretical studies have predicted Rashba splitting in various 2D materials, including transition metal dichalcogenides (TMDCs) and their Janus derivatives [Chhowalla et al., 2013]. Janus TMDCs (formula MXY) are created by replacing one chalcogen atom in a standard TMD (formula MX_2) with a different one, which breaks the structural symmetry and creates a non-uniform charge distribution. This symmetry breaking leads to Rashba-induced spin splitting, especially at the valence band maximum. While some Janus TMDCs like MoSSe have already been synthesized, there is a continued interest in finding new 2D systems to expand the material base for spintronics [Lu et al., 2017]. However, pristine TMDCs often possess intrinsic inversion symmetry, which limits the emergence of the Rashba effect unless external gates or substrates are applied [Zhu et al., 2011].

Recent research has begun to focus on Janus Vanadium Dichalcogenides VXY (X, Y = S, Se, Te), specifically looking at their electronic, magnetic, and structural properties. Although VXY monolayers have not yet been produced in a lab, the successful synthesis of other Janus TMDCs suggests they are experimentally feasible. The advent of Janus monolayers, such as VSTe, has bypassed this limitation by breaking the out-of-plane structural symmetry. By replacing one chalcogen layer with a different atomic species, a built-in vertical electric field is generated, naturally inducing a substantial Rashba effect [Zhang et al., 2017]. Among the emerging Janus materials, Vanadium-based Janus structures stand out due to their unique electronic environment and potential for multifunctional spintronic applications [Dey and Botana, 2020]. Understanding the anisotropy of this Rashba splitting is crucial, as it dictates the spin-precession and spin-texture behavior essential for the realization of the Spin Field-Effect Transistor (s-FET) [Vajna et al, 2012].

Furthermore, mechanical strain engineering has proven to be a powerful tool for modulating the electronic properties of 2D materials [Anshory and Absor, 2020; Anshory and Hanna, 2025]. Given the inherent flexibility of monolayers, applying uniaxial or biaxial strain can significantly alter lattice parameters and bond angles, thereby tuning the SOC strength and the resulting Rashba constant (α_R) [Hu et al., 2018; Affandi et al., 2024]. While several Janus structures like MoSSe or WSSe have been extensively studied [Diery, 2025], a comprehensive understanding of how the anisotropic Rashba effect in Janus VSTe monolayer responds to specific strain configurations remains relatively unexplored in recent literature.

In this study, we employ first-principles calculations based on Density Functional Theory (DFT) and $\vec{k}\cdot\vec{p}$ perturbation theory analysis to systematically investigate the electronic structures and Rashba spin splitting in the Janus VSTe monolayer. We focus on the anisotropy of the spin splitting at the valence and conduction band extrema and explore how these properties can be precisely tuned through uniaxial and biaxial strain. Our findings provide a theoretical foundation for the development of strain-tunable spintronic components based on Janus VSTe monolayer.

2. Research Methods

We utilized the OpenMX software [Ozaki et al., 2009] to conduct DFT calculations under the Generalized Gradient Approximation (GGA) [Perdew et al., 1996]. To achieve precise modeling, we employed norm-conserving pseudopotentials with a 250 Ry energy cutoff for charge density. This specific cutoff value was selected based on the convergence test results shown in **Figure 1(b)**, which demonstrate that the total energy reaches a stable state at this level, consistent with reference [Dey & Botana., 2020; Affandi et al., 2024]. The wavefunction expansion involved a confinement scheme [Ozaki et al., 2004] and a basis set consisting of two s, two p, and one d numerical pseudo-atomic orbitals per atom. Additionally, we accounted for Spin-Orbit Interaction (SOI) via j-dependent pseudopotentials [Theurich and Hill, 2001]. These methods enable a robust investigation into the structural and electronic properties of the studied materials.

Our computational analysis focuses on the Janus VSTe monolayer, specifically the trigonal prismatic 2H-phase, which represents the most stable TMD polymorph at room temperature. The top and side views illustrated in **Figure 1(a)** and **1(b)** highlight the structur of the system. In this arrangement, the central vanadium (V) atom bonds with two different chalcogen atoms, creating a polar, non-centrosymmetric configuration with distinct V–Te and V–S bond lengths. This structure belongs to the C_{3v} point group, providing a necessary foundation for applying $\vec{k}\cdot\vec{p}$ perturbation theory to further explore the material's electronic properties.

Calculations were performed on a periodic slab model of the Janus VSTe monolayer, utilizing a 24 Å vacuum gap to ensure interlayer isolation. We employed an $8 \times 8 \times 1$ k-point grid to sample the Brillouin zone, a configuration selected based on the convergence of total energy as shown in **Figure 2(c)**, and relaxed the atomic geometries to a force tolerance of 1×10^{-5} Hartree/Bohr. As shown in the Brillouin zone map [**Figure 1(a)**], the high-symmetry path includes Γ, M, K, and Q. To analyze the electronic response to mechanical stress, specifically regarding Rashba splitting, we applied uniaxial and biaxial strains [**Figure 1(c)**] from -5% to 5%. Critically, the system was re-optimized at every strain increment to ensure that the reported electronic characteristics reflect the fully relaxed strained geometries.

(a)

(b)

(c)

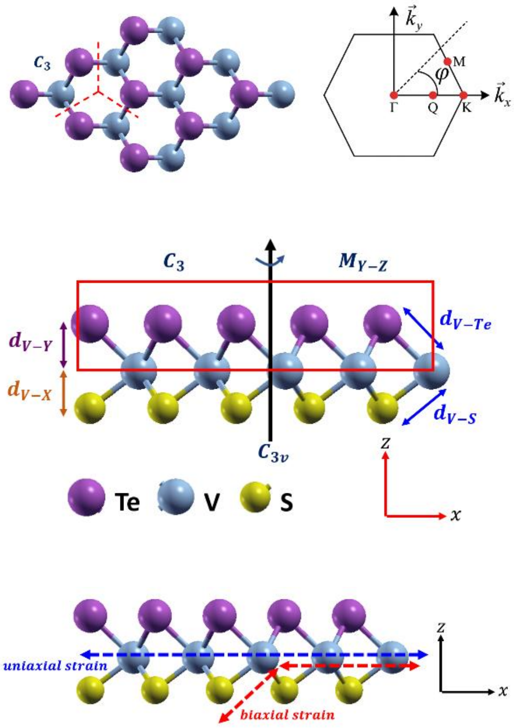

Figure 1. Structural diagrams of the Janus VXY monolayer, visualized using XCrySDen software, are presented in top (a) and side (b) views, detailing vertical atomic separations d_{V-Y} and d_{V-X}, bond lengths d_{V-Te} and d_{V-S}, Panel (a) illustrates the first Brillouin zone within k-space, marking the critical high-symmetry points Γ, M, and K. Panel (c) depicts the application of uniaxial strain in the x-direction and biaxial strain across both the x and y directions.

3. Results and Discussions

Initial structural analysis of the Janus VSTe monolayer yielded an optimized lattice constant of 3.432 Å [**Figure 2a**], consistent with literature. As detailed in **Table 1**, the variation between the V-Te and V-S bond lengths highlights the broken inversion symmetry of the system, identifying it as a non-centrosymmetric crystal structure.

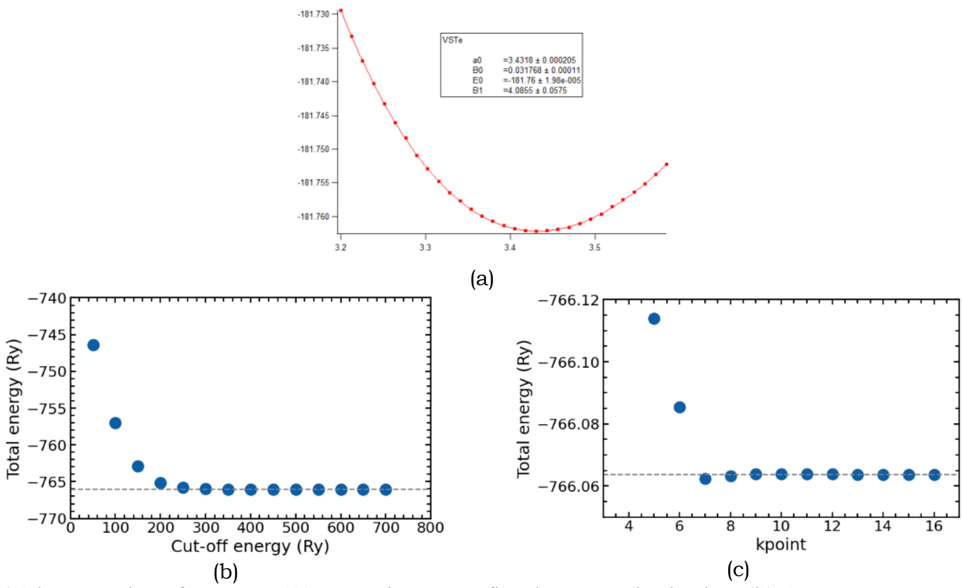

Figure 2. (a) The energies of Janus VSTe monolayer are fitted versus the lattice. (b) Convergence test of the total energy relative to the cut-off energy. (c) Convergence test of the total energy as a function of the k-point grid sampling.

Table 1. The optimized structural parameters of Janus VSTe monolayer systems, including Lattice constant (a), V-chalcogen bonding lengths d_{V-Te} and d_{V-S}, and the distance between two chalcogen atoms (d_{X-Y})

No	a(Å)	d_{V-S}(Å)	d_{V-Te}(Å)	d_{V-X}(Å)	d_{V-Y}(Å)	Ref.
1	3.460	2.33	2.74	1.60	2.17	Dey & Botana., 2020
2	3.432	2.37	2.79	1.64	2.20	Affandi et al., 2024
3	3.432	2.37	2.79	1.64	2.19	This Work

The electronic structure of the Janus VSTe monolayer was subsequently evaluated, with **Figure 3(a)** confirming its semiconducting nature. **Figure 3(b)** illustrates the projected orbital bands for the Janus VSTe monolayer. The valence band maximum (VBM) features two local maxima at the K and Γ points. At the K point, the occupied states are dominated by in-plane atomic orbitals, specifically $d_{x^2-y^2}$ and d_{xy}. In contrast, the states at the Γ point stem from out-of-plane $d_{3z^2-r^2}$ and p_z orbitals, which also facilitate the Rashba splitting observed at this location. Meanwhile, the conduction band minimum (CBM) is located at the K point and is primarily composed of $d_{3z^2-r^2}$ orbital contributions.

The inclusion of spin-orbit interaction (SOI) in our calculations reveals significant Zeeman splitting at the VBM around the K point, a direct result of broken time-reversal symmetry in the Janus VSTe monolayer. However, the more critical feature for this study is the Rashba splitting observed in the VBM near the Γ point. This effect is particularly pronounced in the Janus VSTe system due to the large SOI contributions from S and Te atoms, combined with the inherent lack of inversion symmetry. Such Rashba phenomena align with observations in Janus Mo- and W-based dichalcogenides [Putri et al., 2021], underscoring the necessity of SOI for characterizing these materials for spintronic applications.

Next, the effects of uniaxial and biaxial strain (ranging from -5% to +5% on the Janus VSTe monolayer's electronic structure are examined. This specific range is chosen to avoid structural deformation and aligns with established experimental techniques using substrate-induced strain [Chae et al., 2017]. Strain values are defined by the relation in Eq. (1).

$$\varepsilon_i = \frac{(a_i - a_0)}{a_0} \times 100\% \qquad (1)$$

where a_i and a_0 are the lattice constant of strained and equilibrium structures. **Figure 4** shows the evolution of the band structure of Janus VSTe monolayer with respect to the uniaxial [**Figure 4(a)**] and biaxial [**Figure 4(b)**] strain effect.

(a)

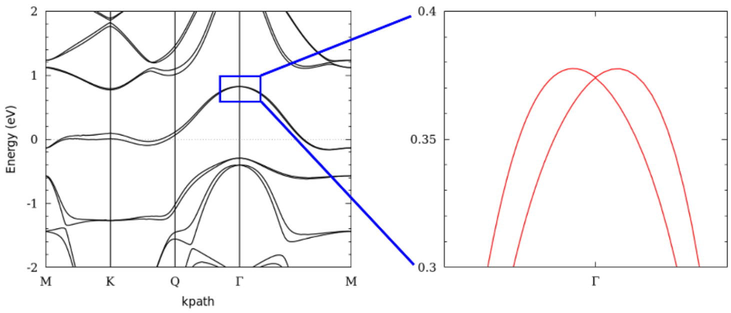

(b)

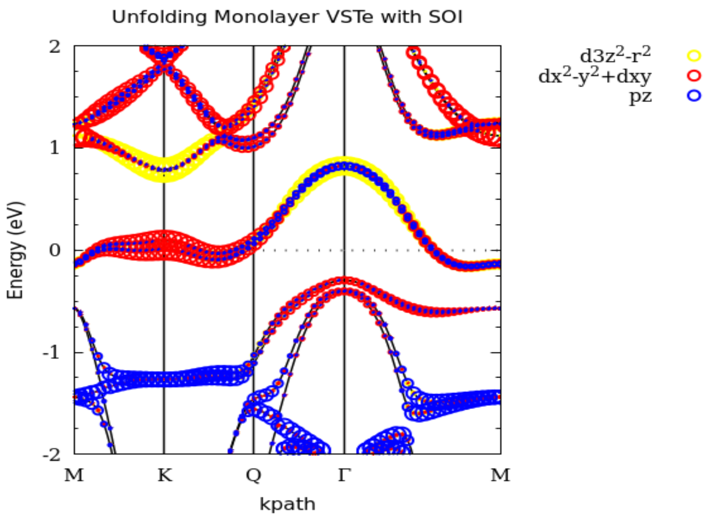

Figure 3. (a) The electronic band structure of Janus VSTe monolayer focusing on magnifications valence band maximum (VBM) around Γ point. (b) Illustrates the projected orbital band (unfolding) of the Janus VSTe monolayer, with colored orbital contributions, and the spectral weights depicted by circle radii.

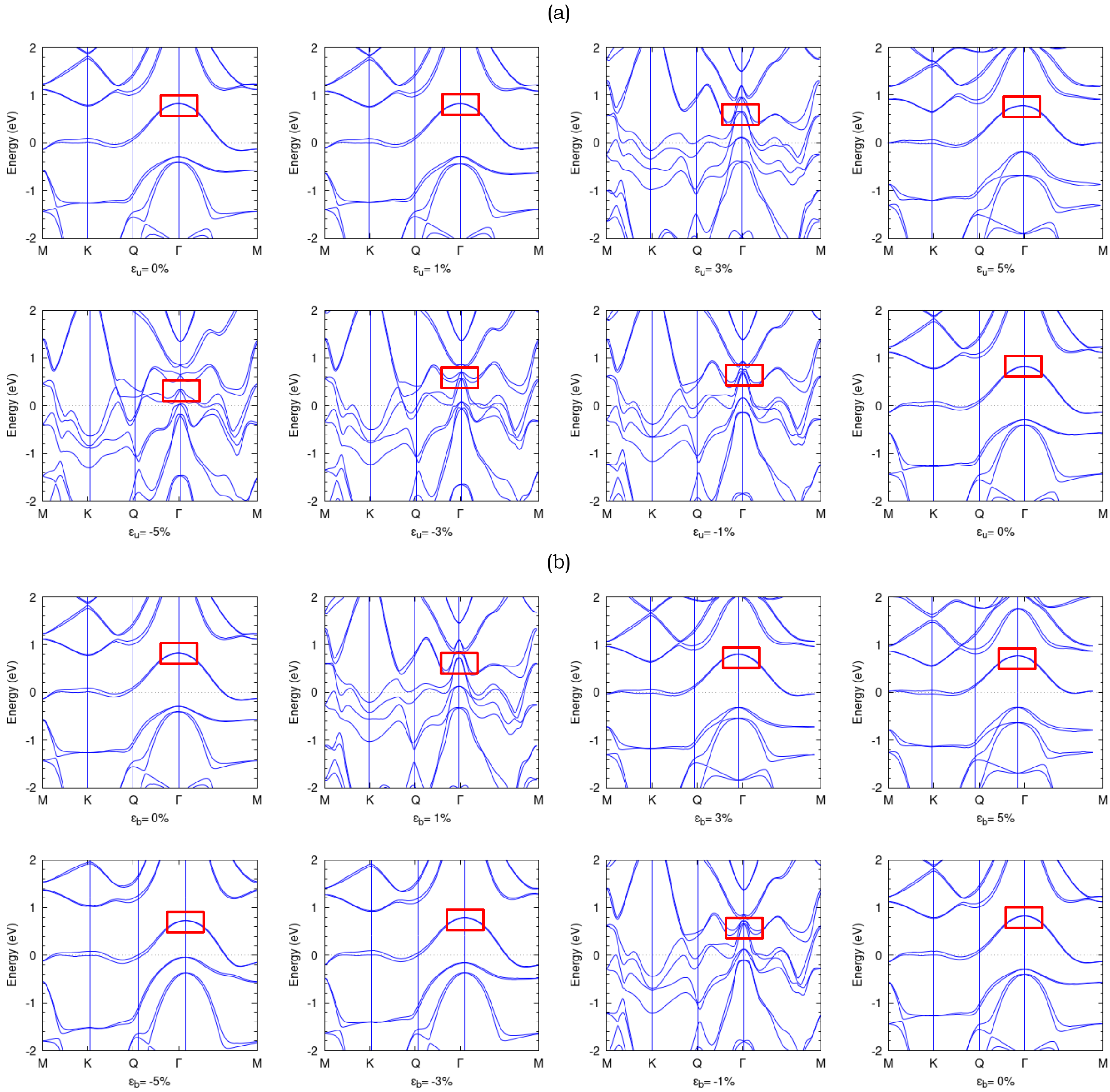

Figure 4. The variation in strain (expansive and compressive strain) induces changes in the electronic structure of the Janus VSTe monolayer : (a) uniaxial and (b) biaxial strain ranging from -5% to +5%. Uniaxial strain induces unstable shifts in the band extrema, leading to band overlap that complicates the Rashba features (red rectangle). Conversely, biaxial strain preserves a stable band profile, ensuring distinct and controllable Rashba splitting.

Under biaxial expansive and compressive strain, the Valence Band Maximum (VBM) shifts from the K point to the Γ point except $\varepsilon = \pm 1\%$ [**Figure 4(b)**]. A similar transition occurs in the Conduction Band Minimum (CBM), which moves from the K point to the midpoint between K and Γ, designated as the Q point. While the indirect nature of the band gap is preserved, the primary optical transition undergoes a significant change from K(CBM)– Γ(VBM) to Q(CBM)–K(VBM). In contrast, the application of uniaxial strain results in band extrema shifts only at expansive strain values of 1% and 5% [**Figure 4(a)**]. These results suggest that the crystal structure of the Janus VSTe monolayer exhibits greater stability when subjected to biaxial strain than when uniaxial strain is applied.

Figure 5 shows the projected orbital bands (unfolding) of the Janus VSTe monolayer due to the application of strain effects. As a result of applying biaxial strain [**Figure 5(b)**], the orbital at the Γ point dominance from out-of-plane $d_{3z^2-r^2}$ and p_z orbitals, which also facilitate the Rashba splitting observed at this location. In contrast, under uniaxial strain [**Figure 5(a)**], an orbital overlap occurs at the Γ point; this suggests a non-semiconducting behavior and the absence of Rashba splitting.

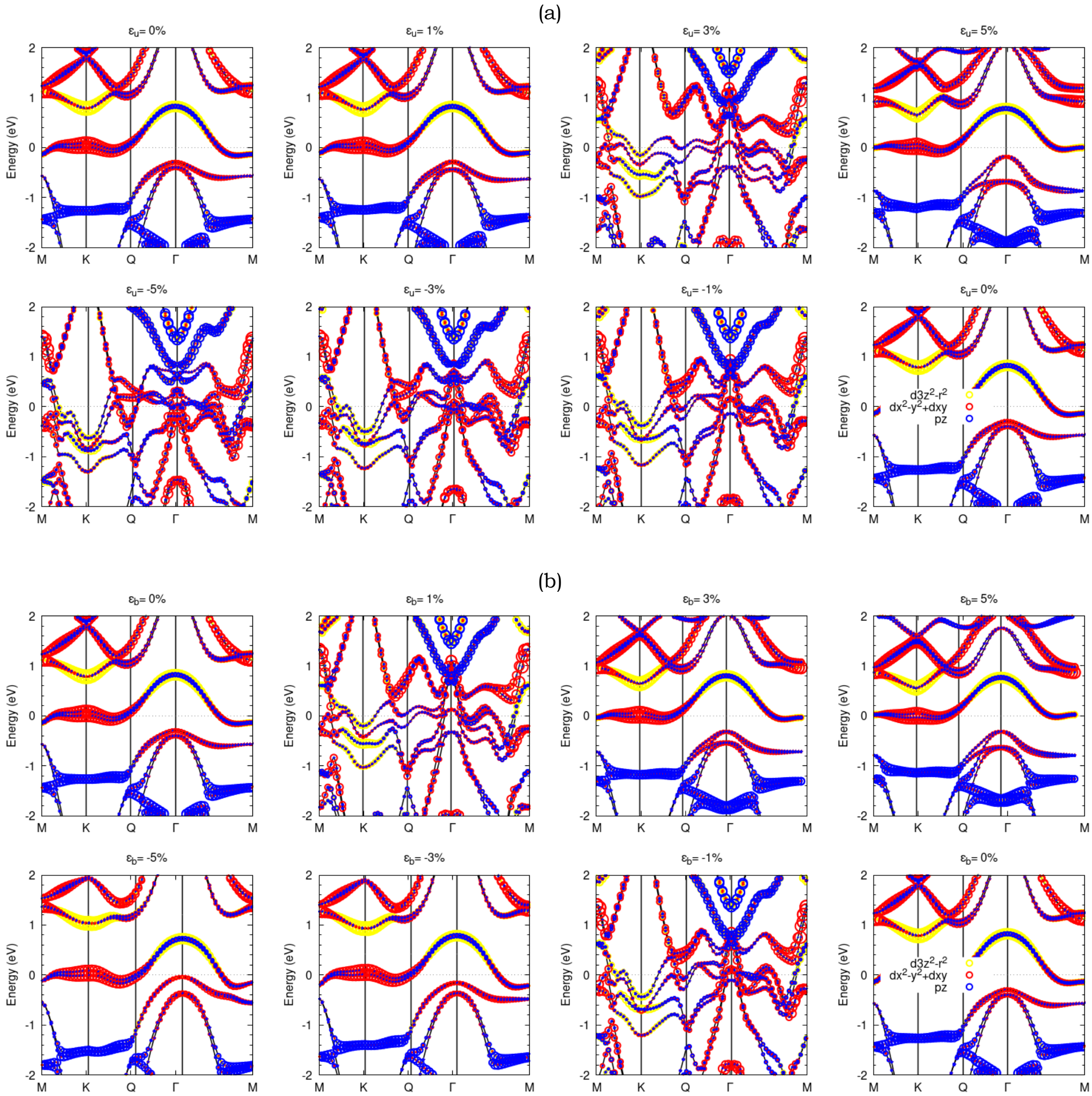

Figure 5. The variation in strain (expansive and compressive strain) induces changes in the projected orbital band (unfolding) of the Janus VSTe monolayer: (a) uniaxial and (b) biaxial strain. The orbital dominance at the Γ point is largely inconsistent under uniaxial strain, whereas it remains notably consistent under biaxial strain, being predominantly dominated by the $d_{3z^2-r^2}$ and p_z orbitals.

The electronic structure of the Janus VSTe monolayer evolves substantially under strain, where biaxial deformation specifically induces a significant modulation of the intrinsic Rashba splitting near the Γ point. This Rashba effect originates from the broken inversion symmetry and the resulting out-of-plane potential gradient inherent to the Janus configuration. By applying biaxial strain, this potential gradient can be precisely tuned through structural adjustments in the d_{V-X} and d_{V-Y} parameters. Consequently, biaxial strain serves as an effective mechanism for manipulating Rashba splitting while maintaining the material's fundamental C_{3v} symmetry.

We analyze the Rashba splitting in Janus VXY monolayers using symmetry-based perturbation theory. Given the C_{3v} crystal symmetry of these monolayers, the Rashba Hamiltonian is derived through an evaluation of the system's irreducible representations. Near the Γ point, the resulting effective Hamiltonian is expressed by Eq. (2) [Sz. Vajna et al., 2012].

$$H(R) = E_0(k) + \alpha(k)\left[\cos(\phi)\,\sigma_y - \sin(\phi)\,\sigma_x\right] + \alpha_3^2 k^3 \cos(3\phi)\,\sigma_z \qquad (2)$$

In this formulation, $E_0(k) = \frac{k^2}{2m^*}$ represents the kinetic energy term governed by the effective mass m^*, while the k-dependent Rashba parameter $\alpha(k)$ incorporates both first-order (α_1) and third-order (α_3^1) contributions. The term α_3^2 accounts for the cubic warping effect. To facilitate analysis in reciprocal space, we define a polar angle $\phi = \cos^{-1}\left(\frac{k_x}{k}\right)$

relative to the k_x axis, which is aligned parallel to the $\Gamma - \mathrm{K}$ high-symmetry direction [**Figure 1**]. From the eigenvalues of the system's Hamiltonian, we derive the squared form of the spin-splitting energy, as detailed in Eq. (3).

$$[\Delta\varepsilon(k)]^2 = (\alpha_1 k + \alpha_3^1 k^3)^2 + (\alpha_3^2)^2 k^6 \cos^2(3\phi) \quad (3)$$

To determine the Rashba parameters of the Janus VSTe monolayer, we performed fitting calculations using Eq. (3) at small k values for various biaxial strain conditions, with the results presented in **Table 2**.

Table 2. Calculated Rashba parameters for the Janus VSTe monolayer under biaxial strain, including first-order and third-order coefficients.

strain	Γ − M		Γ − K		
(%)	α_1(eVÅ)	α_3^1(eVÅ^3)	α_1(eVÅ)	α_3^1(eVÅ^3)	α_3^2(eVÅ^3)
-5	0.020	-0.020	0.025	-0.020	0.050
-3	0.035	-0.040	0.040	-0.030	0.090
-1	0.045	-0.055	0.044	-0.035	0.120
0	0.050	-0.060	0.055	-0.040	0.140
1	0.060	-0.070	0.061	-0.050	0.160
3	0.075	-0.085	0.080	-0.065	0.190
5	0.090	-0.100	0.095	-0.080	0.220

The calculated first order of Rashba parameters (α_1) along the $\Gamma - \mathrm{M}$ and $\Gamma - \mathrm{K}$ symmetry paths are 0.050 eVÅ and 0.055 eVÅ for pristine Janus VSTe monolayer represent a slight departure from earlier literature [Lv et al., 2022]. Furthermore, the results demonstrate that for all investigated biaxial strains, the first order of Rashba parameters (α_1) values along the $\Gamma - \mathrm{M}$ and $\Gamma - \mathrm{K}$ symmetry directions exhibit distinct variations. This discrepancy clearly indicates that the Rashba effect possesses an anisotropic nature. Such behavior suggests that the spin-orbit coupling strength is highly dependent on the momentum direction within the crystal lattice, a finding that aligns with the structural symmetries of the material. This enhancement is primarily driven by the significant SOC contributions arising from the presence of both Sulfur (S) and Tellurium (Te) atoms. Our results extend previous findings by demonstrating that the third-order part contributes significantly to the Rashba parameters. This addition highlights a clear anisotropy in the Rashba effect across the investigated symmetry directions.

Further investigation demonstrates that biaxial strain significantly influences the Rashba splitting in Janus VSTe monolayer, as evidenced by the altered parameter values observed in both the $\Gamma - \mathrm{M}$ and $\Gamma - \mathrm{K}$ directions. As a result of applying 5% expansive biaxial strain, the Rashba parameter values reach 0.090 eVÅ along the $\Gamma - \mathrm{M}$ direction and 0.095 eVÅ along the $\Gamma - \mathrm{K}$ direction. These values are higher than those found in previous research, such as InGaAs/InAlAs (0.070 eVÅ) [Nitta et al., 1998] and the oxide interface $LaAlO_3/SrTiO_3$ (0.01–0.05 eVÅ) [Zhong et al., 2013]. The changes in the Rashba value due to biaxial strain are influenced by our observations that the application of strain markedly influences the difference in distance, denoted as Δz ($\Delta z = |d_{V-X} - d_{V-Y}|$), between S and Te atoms. The change in the Δz value generates a potential gradient, thereby altering the Rashba splitting value.

Unlike standard isotropic Rashba systems that exhibit purely tangential spin orientations, the presence of third-order terms (α_3^1 and α_3^2) in the $\vec{k}\cdot\vec{p}$ Hamiltonian [Eq. 2] induces cubic warping that distorts the constant energy contours into a hexagonal shape. This phenomenon has significant physical implications for electron transport dynamics; the anisotropy of group velocity and direction-dependent spin relaxation will strongly influence the efficiency of spin injection in spintronic devices. Specifically, for Spin-Field Effect Transistor (S-FET) applications, the α_1 value, which can be tuned up to 0.095 eVÅ via 5% biaxial strain, enabling more precise spin precession control over shorter channel lengths and at higher operating temperatures. These findings are critical for designing Spin-FETs, as the magnitude of α_R directly determines the spin precession length ($L_s = \pi\hbar^2/2m^*\alpha_R$).

A crucial finding in this study is the disappearance of Rashba splitting under the influence of uniaxial strain, which differs fundamentally from the stability of Rashba splitting under biaxial strain. Structurally, uniaxial strain along the x-axis [**Figure 1(c)**] breaks the C_3 rotational symmetry, reducing the system's point group from C_{3v} to C_s. This reduction in symmetry triggers significant orbital overlap at the Γ point, as shown in the projected orbital bands [**Figure 5(a)**], resulting in the loss of the semiconductor band gap and the Rashba character of the d_{z^2} and p_z orbitals. This shift causes the out-of-plane potential gradient to no longer effectively separate spin states due to the dominance of distorted inter-orbital interactions. Compared to literature on Janus MoSSe systems where uniaxial strain often only shifts the position of the band extrema, in VSTe, this strain aggressively alters V-S and V-Te orbital hybridization, physically "turning off" the symmetry-protected mechanism for spin splitting.

Compared to oxide interfaces such as $LaAlO_3/SrTiO_3$ [Zhong et al., 2013], which possess relatively small Rashba parameters (0.01–0.05 eVÅ), the VSTe monolayer demonstrates a much more robust responsiveness to strain engineering. This is attributed to the large intrinsic SOC contribution from the heavy Te atoms, combined with the flexibility of the 2D lattice which allows for drastic modulation of Δz without structural failure. Our findings regarding the significant contribution of third-order terms confirm that a linear Rashba description alone is insufficient to model Vanadium-based Janus materials, providing a new dimension in the design of energy-efficient spintronic logic.

Our results contribute significantly to deciphering the complex nature of the Rashba effect in 2D materials. Strain-tunable Rashba effect in Janus VSTe monolayers underscores the significant potential of 2D Janus materials for next-generation spintronics. By demonstrating how lattice strain effectively modulates spin-splitting through structural inversion asymmetry, this study clarifies the fundamental mechanisms of directional anisotropy in these systems. Most importantly, our research provides additional references as candidate materials for Spin-Field Effect Transistor (S-FET) devices, offering a promising platform for the development of high-performance, energy-efficient logic components.

4. Conclusions

Through comprehensive first-principles DFT calculations, we investigated the Rashba splitting effect in Janus VSTe monolayers at the valence band maximum near the Γ point. Using $\vec{k}\cdot\vec{p}$ perturbation theory and symmetry group analysis, we found that the pristine monolayer yields first-order Rashba parameters (α_1) of 0.050 eVÅ along the Γ – M path and 0.055 eVÅ along the Γ – K path, which are effectively modulated by biaxial strain. Under 5% expansive biaxial strain, these values increase to 0.090 eVÅ and 0.095 eVÅ, respectively, surpassing reported values for traditional spintronic interfaces like InGaAs/InAlAs (0.070 eVÅ) and $LaAlO_3/SrTiO_3$ (0.01–0.05 eVÅ). This study provides a unique contribution by demonstrating that third-order terms in the effective Hamiltonian drive the observed directional anisotropy, establishing Janus VSTe monolayer as a superior strain-tunable candidate for high-performance spin-field effect transistors (S-FETs) compared to previously studied transition metal dichalcogenides.

Acknowledgment

This work was supported by HIBAH PENELITIAN ITERA 2025, under grant number 1998ao/IT9.2.1/PT.01.03/2025.

5. Bibliography

Affandi, Y., Absor, M. A. U., Anshory, M., & Amalia, W. (2024). Strong anisotropic Rashba effect with tunable spin-splitting in two-dimensional Janus vanadium dichalcogenides monolayer. *Indonesian Journal of Chemistry, 24*(4), 1184–1194. https://doi.org/10.22146/ijc.93543

Anshory, M., & Absor, M. A. U. (2020). Strain-controlled spin-splitting in the persistent spin helix state of two-dimensional SnSe monolayer. *Physica E: Low-Dimensional Systems and Nanostructures, 124*, Article 114372. https://doi.org/10.1016/j.physe.2020.114372

Anshory, M., & Hanna, M. Y. (2025). The effect of biaxial strain on the thermoelectric properties of 2D SiBi. *Journal of Energy, Material, and Instrumentation Technology, 6*(4), 220–229. https://doi.org/10.23960/jemit.296

Bychkov, Y. A., & Rashba, E. I. (1984). Properties of a 2D electron gas with lifted spectral degeneracy. *JETP Letters, 39*(2), 78–81.

Chae, W. H., Cain, J. D., Hanson, E. D., Murthy, A. A., & Dravid, V. P. (2017). Substrate-induced strain and charge doping in CVD-grown monolayer MoS_2. *Applied Physics Letters, 111*(14), Article 143106. https://doi.org/10.1063/1.4998284

Chhowalla, M., Shin, H. S., Eda, G., Li, L.-J., Loh, K. P., & Zhang, H. (2013). The chemistry of two-dimensional layered transition metal dichalcogenide nanosheets. *Nature Chemistry, 5*(4), 263–275. https://doi.org/10.1038/nchem.1589

Dey, D., & Botana, A. S. (2020). Structural, electronic, and magnetic properties of vanadium-based Janus dichalcogenide monolayers: A first-principles study. *Physical Review Materials, 4*(7), Article 074002. https://doi.org/10.1103/PhysRevMaterials.4.074002

Diery, W. A. (2025). Band gap modulation of a new Janus–non-Janus hybrid MoSSe monolayer: A DFT study. *Physica Scripta, 100*(4), Article 045101. https://doi.org/10.1088/1402-4896/adb8a8

Hu, T., Jia, F., Zhao, G., Wu, J., Stroppa, A., & Ren, W. (2018). Intrinsic and anisotropic Rashba spin splitting in Janus transition-metal dichalcogenide monolayers. *Physical Review B, 97*(23), Article 235404. https://doi.org/10.1103/PhysRevB.97.235404

Lu, A.-Y., Zhu, H., Xiao, J., Chuu, C.-P., Han, Y., Chiu, M.-H., Cheng, C.-C., Yang, C.-W., Wei, K.-H., Yang, Y., Wang, Y., Sokaras, D., Nordlund, D., Yang, P., Muller, D. A., Chou, M.-Y., Zhang, X., & Li, L.-J. (2017). Janus monolayers of transition metal dichalcogenides. *Nature Nanotechnology, 12*(8), 744–749. https://doi.org/10.1038/nnano.2017.100

Lv, M.-H., Li, C.-M., & Sun, W.-F. (2022). Spin-orbit coupling and spin-polarized electronic structures of Janus vanadium-dichalcogenide monolayers: First-principles calculations. *Nanomaterials, 12*(3), Article 382. https://doi.org/10.3390/nano12030382

Manchon, A., Koo, H. C., Nitta, J., Frolov, S. M., & Duine, R. A. (2015). New perspectives for Rashba spin–orbit coupling. *Nature Materials, 14*(9), 871–882. https://doi.org/10.1038/nmat4360

Nitta, J., Akazaki, T., Takayanagi, H., & Enoki, T. (1998). Gate control of spin–orbit interaction in an InAs-inserted $In_{0.53}Ga_{0.47}As/In_{0.52}Al_{0.48}As$ heterostructure. *Physica E: Low-Dimensional Systems and Nanostructures, 2*(1–4), 527–531. https://doi.org/10.1016/S1386-9477(98)00109-X

Ozaki, T., & Kino, H. (2004). Numerical atomic basis orbitals from H to Kr. *Physical Review B, 69*(19), Article 195113. https://doi.org/10.1103/PhysRevB.69.195113

Ozaki, T., Kino, H., Yu, J., Han, M. J., Kobayashi, N., Ohfuti, M., Ishii, F., Ohwaki, T., Weng, H., & Terakura, K. (2009). *OpenMX: Open source package for Material eXplorer*. http://www.openmx-square.org/

Perdew, J. P., Burke, K., & Ernzerhof, M. (1996). Generalized gradient approximation made simple. *Physical Review Letters, 77*(18), 3865–3868. https://doi.org/10.1103/PhysRevLett.77.3865

Putri, S. A., Suharyadi, E., & Absor, M. A. U. (2021). Polarity effect on the electronic structure of molybdenum dichalcogenides MoXY (X, Y = S, Se): A computational study based on density-functional theory. *Indonesian Journal of Chemistry, 21*(3), 598–606. https://doi.org/10.22146/ijc.57949

Rao, Q., Kang, W.-H., Xue, H., Ye, Z., Feng, X., Watanabe, K., Taniguchi, T., Wang, N., Liu, M.-H., & Ki, D.-K. (2023). Ballistic transport spectroscopy of spin-orbit-coupled bands in monolayer graphene on WSe_2. *Nature Communications, 14*(1), Article 6124. https://doi.org/10.1038/s41467-023-41826-1

Theurich, G., & Hill, N. A. (2001). Self-consistent treatment of spin-orbit coupling in solids using relativistic fully separable ab initio pseudopotentials. *Physical Review B, 64*(7), Article 073106. https://doi.org/10.1103/PhysRevB.64.073106

Vajna, S., Simon, E., Szilva, A., Palotás, K., Ujfalussy, B., & Szunyogh, L. (2012a). Theory of spin-orbit coupling-induced anisotropy of the Rashba interaction. *Physical Review B, 85*(7), Article 075302. https://doi.org/10.1103/PhysRevB.85.075302

Vajna, S., Simon, E., Szilva, A., Palotás, K., Ujfalussy, B., & Szunyogh, L. (2012b). Higher-order contributions to the Rashba-Bychkov effect with application to the Bi/Ag(111) surface alloy. *Physical Review B, 85*(7), Article 075404. https://doi.org/10.1103/PhysRevB.85.075404

Zhang, J., Jia, S., Kholmanov, I., Dong, L., Er, D., Chen, W., Guo, H., Jin, Z., Shenoy, V. B., Shi, L., & Lou, J. (2017). Janus monolayer transition-metal dichalcogenides. *ACS Nano, 11*(8), 8192–8198. https://doi.org/10.1021/acsnano.7b03186

Zhong, Z., Tóth, A., & Held, K. (2013). Theory of spin-orbit coupling at $LaAlO_3/SrTiO_3$ interfaces and $SrTiO_3$ surfaces. *Physical Review B, 87*(16), Article 161102. https://doi.org/10.1103/PhysRevB.87.161102

Zhu, Z. Y., Cheng, Y. C., & Schwingenschlögl, U. (2011). Giant spin-orbit-induced spin splitting in two-dimensional transition-metal dichalcogenide semiconductors. *Physical Review B, 84*(15), Article 153402. https://doi.org/10.1103/PhysRevB.84.153402